MICHIGAN STATE UNIVERSITY

CYCLOTRON LABORATORY

A STUDY OF THE $^{194,196,198}Pt(p,p')$ REACTIONS AT 35 MeV

P.T. DEASON, C.H. KING, R.M. RONNINGEN, T.L. KHOO,
F.M. BERNTHAL, and J.A. NOLEN, Jr.

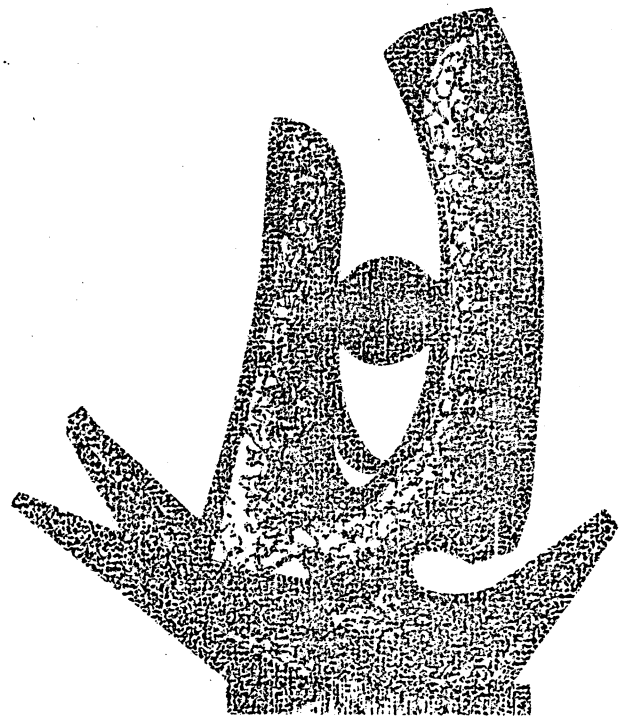

OCTOBER 1980

MSUCL-338

MSUCL-338
October 1980

A study of the ^{194,196,198}Pt(p,p') reactions at 35 MeV

P.T. Deason,* C.H. King,** R.M. Ronningen, T.L. Khoo,+
F.M. Bernthal, and J.A. Nolen, Jr.

Departments of Chemistry and Physics and Cyclotron Laboratory
Michigan State University, East Lansing, Michigan 48824

ABSTRACT

The ^{194,196,198}Pt(p,p') reactions have been studied at a proton energy of 35 MeV using nuclear emulsion plates and a high-resolution position-sensitive proportional counter. Approximately 45 levels were populated in each reaction. In ^{198}Pt, 38 of 44 levels to about 3.2 MeV are reported for the first time. Angular distributions from 20^{o} to 110^{o} were measured for many of these levels. Several new J^{π} assignments were made using empirical shapes of transitions to well-known levels in Pt. The results for the $J^{\pi} = 0^{+}$, 2^{+}, 4^{+}, and (for ^{194}Pt) 6^{+} members of the ground band and the 2^{+}, 3^{+} and 4^{+} members of the "quasi-γ" band were analyzed by coupled channels calculations incorporating relative transition strengths from the interacting boson approximation model. The multipole moments of the deformed optical model potential were calculated and compared to moments deduced from other studies.

Keywords: NUCLEAR REACTIONS ^{194}Pt(p,p'), ^{196}Pt(p,p'), ^{198}Pt(p,p'), E_p = 35 MeV; measured $\sigma(E_p,\theta)$; deduced energies, J^{π}; coupled channels calculations, interacting boson approximation model; deduced optical model and deformation parameters, quadrupole and hexadecapole moments; comparisons to Coulomb excitation, (α,α'), and $(^{12}C, ^{12}C')$; enriched targets, nuclear emulsion plates (7 keV FWHM) and position-sensitive proportional counter (15 keV FWHM), magnetic spectrograph.

I. INTRODUCTION

The transitional region between the well-deformed rare-earth nuclei and the spherical nuclei near ^{208}Pb has been rather intractable to application of traditional models of collective motion. Until recently, most of the properties of the lowest-lying states could be understood only after numerical solution[1,2,3] of the full collective Hamiltonian. Recently a simpler picture, the interacting boson approximation (IBA) model of Arima and Iachello[4] has evolved. This model has its origin in the group symmetry properties of those identical nucleon (or nucleon hole) pairs in angular momentum states of L=0 or L=2 which are outside closed shells. The simplest geometrical models, the vibrational and rotational limits of the collective model, approximately correspond to possible subgroups (SU(5) and SU(3), respectively) for which the IBA Hamiltonian, having SU(6) group symmetry, might be symmetric. In the Os-Pt region the subgroup O(6) has been

plate, at a fixed spectrograph angle. Only the vertical position of the plate in the focal plane was adjusted for each reaction, thus assuring an accurate relative calibration. The data were recorded at 43^{o} and 75^{o} to minimize the interference by the major contaminant reaction peaks, these being due to carbon, oxygen, and silicon. Peak areas and centroids were determined by using the computer code SCOPEFIT.[12] The different reaction kinematics and target thicknesses result in different energy losses so that the energies in ^{198}Pt relative to ^{196}Pt and ^{206}Pb cannot be directly used. Instead, the excitation energy per unit length is measured, this being the same for each spectrum. The energy calibrations of the ^{196}Pt and ^{206}Pb spectra were made by second order polynomial fits to known[13,14] level energies, and also by using a kinematic routine (second order in momentum) to relate the momentum to the distance along the focal plane. Both methods agreed within the experimental uncertainties. The focal plane map was then used to energy calibrate the spectrum for the ^{198}Pt(p,p') reaction at 43^{o} recorded on the plate. The uncertainties in level energies are typically 2 keV below 2.5 MeV excitation energy and 0.1% in energy above 2.5 MeV.

III. EXPERIMENTAL RESULTS

A. General Analysis

Approximately 45-50 levels were populated in each of the three reactions in the region below 3.0 MeV in excitation energy. In the case of ^{198}Pt(p,p'), 38 of the 44 levels observed are

reported for the first time. Only the energies of the first 2^{+} and the second 0^{+} states were accurately known before this study[7,8,9]. The J^{π} assignment for the 0^{+} state was tentative. Tables 1, 2, and 3 summarize the excitation energies, cross sections ($\theta_{Lab} = 30^{o}$) and assignments of J^{π} from the ^{194,196,198}Pt(p,p') reactions. The results from previous studies of these nuclei are included and the results[6] of the ^{196,198}Pt(p,t) reaction studies are shown for comparison.

An attempt was made to assign spin and parity to many of the states seen in each reaction, using the DWBA code DWUCK[29] and standard, collective model form factors. Except for the ground state, and the first 2^{+} level for $\theta \lesssim 50^{o}$, the DWBA calculations provided very poor fits to the data. Thus, the spin assignments were based instead upon comparisons of angular distribution shapes to empirical shapes for states with well-known J^{π}, and from energy and spin systematics in the Pt nuclei.

B. Elastic Scattering and L=0 Transitions

The shape of the elastic angular distributions (Fig. 3) is virtually the same in each reaction. The most notable features at this energy are the "plateau" around 40^{o}, a decrease in cross section of three orders of magnitude within the angular range studied, and three distinct minima between 50^{o} and 100^{o}.

In ^{194}Pt the two states at 1.547 and 1.892 MeV may be the well-known 0^{+} states seen in several decay studies and in the (p,t) reaction study.[6] These states are only weakly populated in the (p,p') reaction, and are not clearly resolved from nearby states in the wire counter data, so no angular distributions

Five states with $J^\pi = 4^+$ were observed in ^{196}Pt, including two which were previously known at 0.876 and 1.293 MeV. A third, at 1.887 MeV, may be the same state seen in the ^{198}Pt(p,t)^{196}Pt reaction[6] (see Table 2) although the energy is 3 keV higher for the state seen in the proton scattering (the energy uncertainties are about 2 keV for each reaction). Two additional states have been tentatively assigned to have $J^\pi = 4^+$, at 2.008 and 2.280 MeV. These states may have been observed in the (p,t) study.[6]

Three states in ^{198}Pt have been assigned to have $J^\pi = 4^+$. The lowest lying one is at 0.984 MeV (0.991 MeV in an (α,α') study[7]). The third 4^+ state is at 1.785 MeV. Thus, three 4^+ states are seen at about 2 MeV excitation in each of ^{192,194,196,198}Pt. The nature of these states is unknown, but their strengths in inelastic proton scattering may indicate a considerable hexadecapole component. This will be discussed below.

F. Transitions with $L \gtrsim 5$

Five L=5 transitions have been assigned on the basis of the empirical shape of the angular distribution for the probable 5^- state at 1.374 MeV in ^{194}Pt (Fig. 5). The 5^- state seen in ^{196}Pt at 1.270 MeV was previously assigned[26] to have $J^\pi = (4,5)^-$ but the (p,t) study[6] preferred $J^\pi = (5^-)$. Assignments of $J^\pi = (5^-)$ were made in ^{194}Pt for levels at 1.932 and 2.165 MeV.

Only one angular distribution (Fig. 5) was obtained for a level known to have $J^\pi = 6^+$, the 1.412 MeV level in ^{194}Pt. The uncertainties are quite large at most angles because of its weak population and its proximity to the strongly populated 3^- level at 1.432 MeV. No attempt was made to extract an angular

distribution for the 6^+ level in ^{196}Pt because the strongly populated 3^- level is only 17 keV away.

Angular distributions were obtained for the 1.485 MeV level in ^{194}Pt and 1.374 MeV level in ^{196}Pt (Fig. 5). The level at 1.485 MeV in ^{194}Pt was previously known to have $J^\pi = 7^-$ from in-beam γ-decay studies,[19] thus affording an empirical shape for comparison in the ^{196,198}Pt(p,p') reactions. The level at 1.374 MeV in ^{196}Pt had been previously assigned as $(6^+,7^-)$, but its angular distribution suggests $J^\pi = 7^-$. An assignment of $J^\pi = (6^+,7^-)$ has also been made for the level at 1.502 MeV in ^{198}Pt. A level at 1.722 MeV in ^{198}Pt could not be given an assignment because of its weak population.

Figure 5 includes twelve seemingly unique angular distributions, three from ^{194}Pt, four from ^{196}Pt, and five from ^{198}Pt, all with essentially the same features, the most prominent of which is a strong maximum at 50° on an otherwise smoothly decreasing cross section. The levels are at relatively high excitation energies, from 2.1 to 2.8 MeV. The transitions to them are some of the strongest in each reaction. Unfortunately there are no known levels in any of the reactions with a similar shape, so no spin information can be obtained. However, the strength of these transitions and their high excitation energy (approximately 1 MeV above the pairing gap at about 1.4 MeV) may indicate these states are composed of highly correlated, particle-hole configurations. Further investigation is needed, though, before a definite characterization of these states can be made.

Several additional angular distributions are shown in Fig. 6. No spin assignments were made for these transitions because of large uncertainties in the angular distribution data.

included couplings between the 0^+, 2^+, and 4^+ levels. The parameter search was conducted by simultaneously varying either the three potential depths (V, W_D, V_{SO}) or the diffuseness parameters (a_R, a_I). The sequence of searches typically involved two iterations of a search on the well depths followed by a search on the diffuseness parameters, one search on the deformation parameter, β_2, while minimizing $\chi^2_{2^+}$, then two more iterations on (V, W_D, V_{SO}) and (a_R, a_I). The starting β_λ values were deduced from values in Ref. 7. The Coulomb and nuclear matrix elements are assumed to have the same relative values (discussed below) although each set is normalized to the $0^+ \rightarrow 2^+$ and $0^+ \rightarrow 4^+$ matrix elements which are calculated in ECIS from the DOMP. All the calculations were performed using 25 partial waves, an integration step size of 0.33 fm, and a matching radius of 20 fm. The multipole expansion included couplings of $\lambda = 2$ and $\lambda = 4$ terms to L=8. For simplicity, the nuclear deformations were equal for the real and the imaginary portions of the potential.

The search results are given in Table 4 for calculations employing a deformed full Thomas form[34] for the spin-orbit term (L*S), and for calculations without a spin-orbit (L*S = 0), as discussed below. The changes in the parameters from Becchetti-Greenless parameters[33] when L*S $\neq$ 0 are relatively small except for values of the real diffuseness, a_R, and the imaginary surface term, W_D. These decrease by about 7% and 12%, respectively.

B. The IBA Matrix Elements

Since relatively little is known about the matrix elements which connect the low-lying states of the Pt nuclides (except[35]

in the case of ^{194}Pt), one must use a nuclear structure model which makes predictions of matrix elements. This allows a test of the predictive qualities of the nuclear structure model beyond comparisons of energy levels and transition rate ratios. With the recent success of the O(6) limit of the IBA in the Pt-Os region for energy levels, E2 branching ratios,[5] and (p,t) strengths,[6] the coupled channel analysis of the (p,p') reaction should provide a natural framework for further testing the E2 and E4 matrix elements. We note that our data on ^{194}Pt could not be well described[36] using simple collective models.

The matrix elements used in the analysis were obtained from the computer code PHINT[37] which diagonalizes the IBA Hamiltonian. We use a "perturbed" O(6) Hamiltonian. In the O(6) limit the eigenvalues are given by

$$E(N, \sigma, \tau, \nu_\Delta, J) = \frac{A}{4}(N-\sigma)(N+\sigma+4) + B_\tau(\tau+3)+CJ(J+1),$$

where A, B, and C are constants, N is the number of bosons, and σ, τ, ν_Δ, and J are quantum numbers (see Ref. 5 for a detailed discussion). Deviations from this limit can be introduced by including a term for the quadrupole-quadrupole interaction between bosons,[5] whose strength is given by κ. It should be noted that the introduction of this term is still within the context of the IBA model and only requires[4] a more complete solution of the full IBA Hamiltonian.

Small values of κ primarily affect the magnitude of transitions which are not allowed in the strict O(6) limit because of the $\Delta\tau = 1$ selection rule. The matrix elements most affected are $M_{02'}$, M_{23}, $M_{24'}$, $M_{34'}$, and $M_{2'4'}$ where

D. Sensitivity of CC Calculations to Higher Order Couplings and Selected Matrix Elements

1. The Sign of β_4

Earlier theoretical calculations (e.g. Ref. 38) and experiments[7,39] have indicated a negative value of β_4 for the Pt nuclides. A series of calculations were performed to investigate the sensitivity of the (p,p') data to the sign of β_4. Figure 8 compares the result of a $0^{\pm}2^{\pm}4^{\pm}6^{+}$ calculation for ^{194}Pt with a positive, negative, and zero value for β_4. This calculation included the spin-orbit interaction. Using a negative β_4 value, the overall slope and the fit to the first maximum are in agreement with the data. The oscillations for a positive value of β_4 (dashed line fit in Fig. 8) are almost completely out of phase with those for $\beta_4 = 0$, and the cross section is overestimated at backward angles. Also, the value of $\chi^2_{2^+}$ increases by a factor of 2. The calculation with $\beta_4 = 0$ clearly fails to reproduce the data. The necessity of including a β_4 component is also discussed in section C.-6., concerning the second 4^+ level. The present results support earlier findings[7,39] of a negative value of β_4 for the Pt isotopes. Although there might be evidence[40] in the rare-earth region for small values of β_6 this was not investigated.

2. The Effect of the "Quasi-γ" Band Couplings

In order to test further the O(6) IBA matrix elements, calculations were performed including the lowest states of the "quasi-gamma" band, whose bandhead is the second 2^+ state. Three previous inelastic scattering studies of the Pt nuclei have also

studied members of this band. These states are the $2^{+\prime}$, 3^+, and $4^{+\prime}$ states in ^{194,196}Pt and the $2^{+\prime}$ and $4^{+\prime}$ states in ^{198}Pt. The calculations included both β_2 and β_4 deformations, the IBA matrix elements in Table 6, and $L^*S \neq 0$. The IBA $0 \rightarrow 4^{+\prime}$ matrix element relative to that for $0^+ \rightarrow 4^+$ is extremely small and a larger value was necessary to reproduce the data.

The results of these calculations for ^{194}Pt are shown in Fig. 9 for two different sets of matrix elements. One set was calculated using PHINT,[34] the parameters of Ref. 5, and $\kappa = 0.0375$ keV. The second set was calculated using $\kappa = 0.5375$ keV. This larger value of κ gives a value for $B(E2; 2^{+\prime} \rightarrow 0^+)/B(E2; 2^{+\prime} \rightarrow 2^+)$ closer to the experimental one than when $\kappa = 0.0375$ keV. The calculations fit better the angular distribution for the $2^{+\prime}$ state, but at the expense of the already poorly fit 3^+ and $4^{+\prime}$ state data. The value of κ=0.5375 keV is almost twenty times larger than that used in Ref. 5, but it is not unrealistically large. In fact, values in the Os region[5] are an order of magnitude still larger than those in the Pt region.

3. The Effect of the $2^{+\prime}$ State on the β_λ Values

To test the influence the $2^{+\prime}$ state may have on extracting the deformation parameters, a search was made on β_2 and β_4 simultaneously using 0^+-2^+-4^+-$2^{+\prime}$ level couplings and the IBA matrix elements with $\kappa = 0.5375$ keV. The χ^2 values were minimized for each level. Similarly, a search was made using 0^+-$2^{\pm}4^+$-6^+ level coupling. Both calculations used the same initial values for β_2 and β_4, and in each calculation, χ^2_T ($= \chi^2_0 + \chi^2_2 + \chi^2_4$) minimized for the same final values within statistical undertainties.

used (except for ^{198}Pt where no 3^+ couplings were included). The shapes of the $4^{+\prime}$ angular distribution with and without the spin-orbit couplings are similar. The results of these calculations are shown as the solid curves in Fig. 11 for ^{194,196,198}Pt. The best fit for the $4^{+\prime}$ angular distribution is obtained in the ^{198}Pt case, with the rather structureless shape except for a maximum at 35^{o}. The other three calculations show considerably more diffraction for this angular distribution. Table 8 summarizes the M_{04}' and B(E4) values as well as these values from the ^{192}Pt(α,α') reaction.[39] Baker et al.[39] obtained a better fit to their data with a positive value for M_{04}'; our values are negative for ^{194}Pt and positive for ^{196,198}Pt. However, these matrix elements depend on the two-step and three-step excitation routes to the $4^{+\prime}$ level, leading to an uncertainty in value as is shown in Table 8 for ^{192}Pt. The best fit values obtained in this study are thus significant only for the values of M_{02}, M_{22}', $M_{2\ 4}'$, and M_{02}'.

E. Comparison of Charge and Nuclear Potential Moments

Mackintosh,[44] using a theorem by Satchler,[45] has shown that the multipole moments of the real part of the deformed optical model potential (DOMP) are proportional to the moments of the nuclear matter density, if the DOMP for protons is derivable from a reformulated optical model potential. This assumes that the nucleon-nucleon interaction is independent of density, and that the proton and neutron distributons have equal deformations. The multipole moment method is a more fundamental approach to compare results from Coulombic and hadronic scattering experiments.

The β_λ, or the "deformation lengths" $\beta_\lambda R$, where R is the potential radius, are reaction dependent quantities. Inelastic nucleon scattering cross sections depend on the product $\beta_\lambda R$ whereas Coulomb excitation cross sections are proportional to the squares of the Eλ matrix elements, which have a first order $\beta_\lambda R^\lambda$ dependence. The product $\beta_\lambda R$ may also be correlated with other optical model parameters.

Following the suggestion by Mackintosh, the multipole moments q_2 and q_4 were calculated from the real part of the DOMP using the relation

$$q_\lambda = \frac{K\int V(\vec{r}) r^\lambda Y_{\lambda o}(\theta) d\vec{r}}{\int V(\vec{r}) d\vec{r}}$$

The DOMP parameters are those given in Tables 4 and 7. When K is chosen to be equal to Z, the proton number, the comparison can be made with results from electromagnetic excitation studies. The moments from our study are given in Table 9 along with moments from Coulomb excitation[33,41,46] and those calculated from the DOMP and Coulomb potentials used in an (α,α') reaction study.[7] The Coulomb deformation parameters obtained in Ref. 40 and Ref. 7 are those for a uniform charge distribution with a sharp cutoff, for asymmetrically and symmetrically deformed shapes, respectively. The potential moments in the present study and in Ref. 7 are for a deformed Fermi distribution.

A comparison of the (p,p') results with those from the previous experiments indicates the q_2 potential moments from proton scattering are in much better agreement with the charge moments from Coulomb excitation than are the potential moments of Baker

fit only by allowing a direct L=4 excitation of this state. The sensitivity of the calculations to several effects was noted: the sign of the L=2 matrix element product which connects the $J^{\pi} = 0^{+}$, 2^{+} and $2^{+\prime}$ levels; the quadrupole strength parameter, κ, in the IBA model; and the effect of the quasi-γ band on the extraction of the moments. The extracted moments are systematically more negative but are in better agreement with values from Coulomb excitation than are the moments derived from the DOMP parameters used in (α,α') studies.

ACKNOWLEDGMENTS

We wish to express our gratitude to Drs. R.F. Casten, J.A. Cizewski, S.W. Yates, and J.P. Delaroche for their interest in our study, and for helpful discussions with us. We are indebted to Dr. J. Raynal for his code ECIS and for communications pertaining to its use. This material is based upon work supported by the National Science Foundation under Grant No. Phy 78-22696.

* Present address: E.I. DuPont Corp., Savannah River Plant, Aiken, SC 29801

** Present address: Bell Laboratories, Murray Hill, NJ 07974.

+ Present address: Physics Division, Argonne National laboratory Argonne, IL 60439

1. G. Gneuss and W. Greiner, Nucl. Phys. A171, 449 (1971).
2. T. Kishimoto and T. Tamura, Nucl. Phys. A192, 246 (1972), Nucl. Phys. A270, 317 (1976).
3. Krishna Kumar and Michel Baranger, Nucl. Phys. 122, 273 (1968).
4. A. Arima and F. Iachello, Ann. Phys. (N.Y.) 99, 253 (1976), Ann. Phys. (N.Y.) 111, 201 (1978), A. Arima and F. Iachello, Ann. Phys. 123,468 (1979), Phys. Rev. Lett. 40, 385 (1978).
5. J.A. Cizewski, R.F. Casten, G.J. Smith, M.L. Stelts, W.R. Kane, H.G. Borner and W.F. Davidson, Phys. Rev. Lett. 40, 167 (1978), R.F. Casten and J.A. Cizewski, Nucl. Phys. A309, 477 (1978).
6. P.T. Deason, C.H. King, T.L. Khoo, J.A. Nolen, Jr., and F.M. Bernthal, Phys. Rev. C20, 927 (1979).
7. F.T. Baker, Alan Scott, T.H. Kruse, W. Hartwig, E. Ventura, and W. Savin, Nucl. Phys. A266, 337 (1976).
8. E.J. Bruton, J.A. Cameron, A.W. Gibb, D.B. Kenyon, and L. Keszthelyi, Nucl. Phys. A152, 495 (1970).
9. Paresh Mukherjee, Nucl. Phys. 64, 65 (1965).
10. R.G. Markham and R.G.H. Robertson, Nucl. Instr. Meth. 129, 131 (1975).
11. H.G. Blosser, G.M. Crawley, R. Deforest, E. Kashy, and B.H. Wildenthal, Nucl. Instr. Meth. 91, 61 (1971).

Table 1. States populated in the ^{194}Pt(p,p') reaction with comparisons to results from the ^{196}Pt(p,t) reaction and other studies.

Present Experiment ^{194}Pt(p,p')			Previous Results ^{196}Pt(p,t)^{194}Pt[a]		Other results[b]
E_x (MeV)	J^π	$\sigma(30^\circ)$ (μb/sr)	E_x[c] (MeV)	E_x (MeV)	J^π	J^π
0.0	0^+	5.00×10^5	0.0	0.0	0^+	0^+
0.328	2^+	5.03×10^3	0.3285	0.328	2^+	2^+
0.622[d]	2^+	167	0.6221	0.622	2^+	2^+
0.811[d]	4^+	328 (40°)	0.8112	0.811	4^+	4^+
0.922(2)	(3^+)	26.6	0.9228			3^+
1.229[d]	4^+	158	1.2295	1.229	4^+	4^+
			1.2671	1.267	0^+	0^+
1.374[d]	5^-	77.5	1.3734	1.374	$(4^+,5^-)$	(5^-)
1.412	6^+	36.1	1.4116	1.414(2)	6^+	6^+
1.432[d]	3^-	1.34×10^3	1.4325	1.433	3^-	3^-
			1.4792	1.479(2)	0^+	0^+
1.485[d]	7^-	66.5	1.4853	1.486(2)		7^-
1.511(3)			1.5119	1.512(3)		2^+
1.529(2)						
1.547			1.5472	1.547	0^+	0^+
1.670	(2^+)	11.0 (40°)	1.6706	1.670		2^+
1.736		28.3				
			1.7787	1.778		$(1,2,3)^+$
1.796		38.6	1.7974			1^-
1.815		14.8	1.817	1.815		(3^-)
1.870		123				
1.892[d]			1.8936	1.892		0^+
1.911[d]	(4^+)	457		1.911	(4^+)	
1.932	(5^-)	141	1.9302	1.931		$(1,2,3)^+$
1.948(3)		37.6	1.9485	1.947		
1.974						
1.981		22.1				
			1.9917	1.990	$(6^+,7^-)$	
			1.9999	2.001		(8^-)
2.030		33.5	2.03	2.031		
			2.0638	2.062		(2^+)
2.072		120				
2.104		37.0		2.105		
2.126	(4^+)	105	2.13	2.125	(4^+)	

42. A.S. Davydov and G.F. Fillippov, Nucl. Phys. 8, 237 (1958).
43. K. Kumar, Phys. Lett. 29B, 25 (1969).
44. R.S. Mackintosh, Nucl. Phys. A266, 379 (1976).
45. G.R. Satchler, J. Math. Phys. 13, 1118 (1972).
46. J.E. Glenn, R.J. Pryor, and J.X. Saladin, Phys. Rev. 188, 1905 (1969).
47. R.F. Casten, private communication.

Table 2. States populated in the ^{196}Pt(p,p') reaction with comparisons to results from the ^{198}Pt(p,t) reaction and other studies.

Present Experiment ^{196}Pt(p,p')			Previous Results ^{198}Pt(p,t)^{196}Pt[a]		Other Results[b]	
E_x (MeV)	J^π	$\sigma(30^o)$ (μb/sr)	E_x (MeV)	J^π	E_x[c] (MeV)	J^π
0.0	0^+	5.69×10^5	0.0	0^+	0.0	0^+
0.356	2^+	4.55×10^3	0.356	2^+	0.3557	2^+
0.689[d]	2^+	48.7(40^o)	0.689	2^+	0.6889	2^+
0.877[d]	4^+	258	0.877	4^+	0.8770	4^+
1.014(2)	3^+	9.88(45^o)			1.0152	3^+
			1.135	0^+	1.1352	0^+
1.270[d]	(5^-)	180	1.271	5^-	1.2705	$(4,5)^-$
1.293[d]	(4^+)	269	1.293	(4^+)		
			1.362		1.3617	$(1^+,2^+)$
1.374[d]	7^-	104	1.374	$(6^+,7^-)$	1.374	$(6,7)^-$
			1.402	0^+	1.4027	$0^+,1^+,2^+$
1.447	3^-	1.08×10^3	1.447	3^-	1.4471	3^-
1.529		77.0	1.527			
			1.537			
1.603(3)	2^+	29.8	1.606	(2^+)	1.6045	$0^+,1,2^+$
1.679(3)		32.9	1.675(3)		1.677	2^+
1.756(3)		37.7			1.7546	$3,4^\pm,5^-$
			1.796			
1.826(3)		67.8	1.824	0^+	1.8234	0^+
			1.848	(2^+)	1.8471	$0^+,1,2$
1.887	4^+	536	1.884	(4^+)	1.88	
1.964(3)			1.932			
			1.987			

Table 2. con't.

Present Experiment ^{196}Pt(p,p')			Previous Results ^{198}Pt(p,t)^{196}Pt[a]		Other Results[b]	
E_x (MeV)	J^π	$\sigma(30^o)$ (μb/sr)	E_x (MeV)	J^π	E_x[c] (MeV)	J^π
2.008	(4^+)	295	2.006			
2.055(3)			2.052			
			2.072			
			2.095			
2.116		179	2.114			
2.129		291	2.128		2.1289	$1^-,2^+$
			2.164		2.1627	$0^+,1,2$
2.179			2.174		2.1744	2^+
			2.193		2.1908	$0^+,1,2$
			2.204		2.2044	2^+
2.243		48.6			2.2455	$(1,2)^+$
			2.264		2.2641	$1,2^+$
2.280	(4^+)	65.0	2.277			
			2.296	$(7^-,8^+)$		
2.305		50.0			2.3092	$(1,2)^+$
2.331(4)						
2.349					2.3453	$1^+,2^+$
2.360						
			2.370			
			2.386			
2.393					2.39	
			2.423			
2.431		541				

Table 3. States populated in the ^{198}Pt(p,p') reaction.

Present Experiment ^{198}Pt(p,p')			Previous Results[a]	
E_x[b] (MeV)	J^π	$\sigma(30^o)$ (μb/sr)	E_x[b] (MeV)	J^π
0.0	0^+	4.92×10^5	0.0	0^+
0.407[c]	2^+	3.24×10^3	0.4072	2^+
0.775	2^+	55.1(40^o)	0.775	2^+
0.984	4^+	1.05×10^3	0.991	4^+
1.246(3)	(3^+)	21.9		
1.287	4^+	252	1.305	
1.367	(5^-)	142		
1.445(3)		56.6		
1.502(3)	(7^-)	82.8		
1.657		119		
1.682	3^-	845		
1.722(3)		25.5(40^o)	1.722	(3^-)
1.785	(4^+)	150		
1.827(4)				
1.900		113		
1.949				
1.971(4)				
2.000				
2.070		46.6(40^o)		
2.100		74.9		
2.120		57.9		
2.155		137		
2.178		52.7		
2.319				
2.339				

Table 3. (cont'd.)

Present Experiment ^{198}Pt(p,p')			Previous Results[a]	
E_x[b] (MeV)	J^π	$\sigma(30^o)$ (μb/sr)	E_x[b] (MeV)	J^π
2.356				
2.387				
2.441		369		
2.469		49.9		
2.514		108		
2.573		36.3	2.53	
2.611		762		
2.633				
2.666		96.5		
2.726		62.3		
2.782				
2.796		325		
2.826		385		
2.884		38.4		
2.910		38.0		
3.005				
3.018				
3.170(5)				
3.197(5)				

[a] References 7, 8, 9.

[b] Uncertainties in the excitation energies are approximately 2 keV below 2.5 MeV and 0.1% above 2.5 MeV, except where indicated.

[c] Used as calibration point along with the 0.80310, 6.68408, 2.20023, and 2.64790 MeV levels from ^{206}Pb (Ref. 28).

Table 6. Relative matrix elements for $^{194,196,198}Pt$ calculated using the O(6) symmetry in the IBA model

r	s	^{194}Pt κ = 0.0375keV $-M_{rs}(E2)$	$M_{rs}(E4)$	^{194}Pt κ = 0.5375keV $-M_{rs}(E2)$	$M_{rs}(E4)$	^{196}Pt κ = 0.025keV $-M_{rs}(E2)$	$M_{rs}(E4)$	^{198}Pt κ = 0.016keV $-M_{rs}(E2)$	$M_{rs}(E4)$
0	2_1	-1.0		-1.0		-1.0		1.0	
0	2_2	0.0046		0.0627		0.00242		-0.00123	
0	4_1		1.0		1.0		1.0		1.0
0	4_2		-0.00267		0.0369		-0.00131		-0.0006
2_1	2_1	-0.0142	1.380	-0.196	1.376	-0.0073	1.436	-0.0035	1.521
2_1	2_2	-1.156	-0.00370	-1.142	-0.0508	-1.144	-0.0020	-1.127	-0.0011
2_1	4_1	1.551	-0.0152	1.552	-0.209	-1.535	0.0081	-1.512	0.00415
2_1	3	-0.0061	0.559	-0.0838	0.557	0.00314	-0.544		
2_1	4_2	0.0011	0.818	-0.0155	-0.802	0.0006	0.797	-0.00036	-0.763
2_1	6		-1.426		-1.425		-1.388		-1.329
2_2	2_2	0.0142	0.656	0.196	0.659	0.0073	0.694	0.00353	0.751
2_2	4_1	0.0029	-1.721	-0.0397	1.269	0.0016	1.818	0.00085	1.970
2_2	3	-1.186	-0.00359	-1.186	-0.0494	1.155	0.0017		
2_2	4_2	-1.152	-0.0152	1.155	0.210	-1.121	-0.00795	1.073	0.00398
4_1	4_1	-0.0127	0.0878	-0.175	0.883	-0.0063	0.927	-0.00295	1.004
4_1	3	0.750	-0.00399	0.0748	0.00551	0.730	-0.0023		
4_1	4_2	1.098	-0.00572	-1.090	0.0787	-1.069	0.0030	1.024	-0.00156
4_1	6	-1.913	0.0130	-1.914	0.180	1.862	0.0069	1.783	-0.00346
4_1	8		-1.622						
3	3		-1.767		-1.765		1.901		
3	4_2	0.00742	-0.748	0.103	0.744	-0.0064	0.804		
3	6		-1.452		1.446		1.564		
4_2	4_2	0.00694	1.525	0.0949	1.512	0.0036	1.641	0.00179	1.820
6	6	-0.0101	0.965	-0.141	0.969	-0.0048	1.038	-0.00204	1.152
6	8	2.120	-0.011						
8	8	-0.00752	1.133						

Table 7. Deformation parameters and potential moments obtained from $0_1^+ 4_1^+ 6^+$ coupled channel calculations for $^{194,196,198}Pt$. Values from calculations with (L*S) and without (L*S=0) a spin-orbit interaction are included.

Nucleus	β_2	β_4	q_2 (b)	q_4 (b^2)
^{194}Pt				
κ = 0.0375[a]				
L*S	-0.154(2)	-0.0455(10)	-1.32(2)	-0.156(7)
L*S = 0	-0.168(3)	-0.0566(17)	-1.40(2)	-0.184(12)
κ = 0.5375				
L*S	-0.151(2)	-0.0453(10)	-1.30(2)	-0.160(6)
L*S = 0	-0.164(3)	-0.0550(20)	-1.37(3)	-0.181(12)
^{196}Pt				
κ = 0.025				
L*S	-0.142(3)	-0.0485(13)	-1.25(3)	-0.202(11)
L*S = 0	-0.152(5)	-0.0573(21)	-1.31(5)	-0.226(16)
^{198}Pt				
κ = 0.016				
L*S	-0.119(2)	-0.0422(20)	-1.05(2)	-0.177(7)
L*S = 0	-0.128(4)	-0.0479(30)	-1.09(4)	-0.181(18)

[a]The unit for κ is keV.

Table 9. (cont'd.)

Nuclide	Method	q_2^a (b) or (eb)	q_4^a (b^2) or (eb^2)
^{198}Pt			
	(p,p') at 35 MeV[b]	-1.05(2)	-0.177(7)
	Coulomb excitation[f]	-1.00(3)	
	(α,α')[e] P	-1.12	-0.32
	C	-1.08	-0.14

[a] The units for the charge component moments are b^λ, λ = 2 or 4. The units for the electromagnetic moments are eb^λ.

[b] These moments were obtained using the DOMP parameters, including the spin-orbit interaction, contained in Tables 4 and 7.

[c] Ref. 35.

[d] Ref. 41.

[e] Ref. 7. The first value reported is the potential moment (P) and the second value is the charge distribution moment (C).

[f] Ref. 46.

Figure Captions

FIG. 1. Inelastic scattering proton spectra for the ^{194,196,198}Pt(p,p' reactions at 35 MeV. The data were obtained with nuclear emulsion plates. The elastic scattering peaks are not shown because they were too dense to scan. Peaks marked with "*" indicate that either the peak height has been cut off at the maximum value on the vertical axis or was unscannable.

FIG. 2. Inelastic scattering proton spectra for the ^{194,196,198}Pt (p,p') reactions at 35 MeV. The data were obtained with a delay-line proportional counter.

FIG. 3. Elastic scattering and L=0, 2 angular distributions from the ^{194,196,198}Pt(p,p') reactions. The curves are the results of DWBA calculations using a collective model form factor. Energies are given in keV.

FIG. 4. L=3, 4 angular distributions from the ^{194,196,198}Pt (p,p') reactons. Energies are given in keV.

FIG. 5. $L \geq 5$ angular distributions from the ^{194,196,198}Pt(p,p') reactions. In the third and fourth panels are angular distributions with unique shapes unlike those for levels with known J^π. Energies are given in keV.

FIG. 6. Angular distributions from the ^{194,196,198}Pt(p,p') reactions with unknown L transfer. Energies are given in keV.

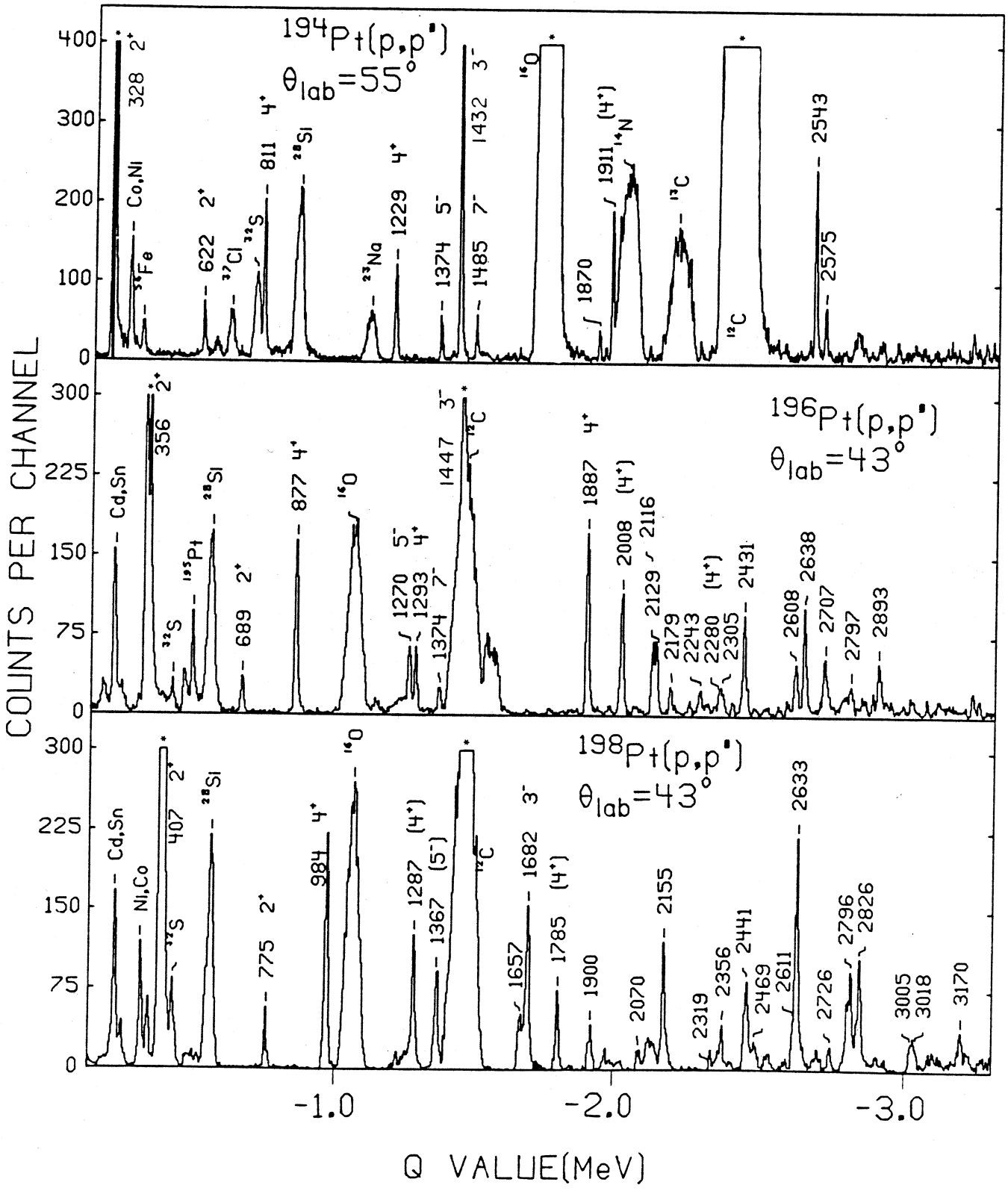

"A Study of the $^{194,196,198}Pt(p,p')\ldots$," P.T. Deason et al. Fig. 1 .

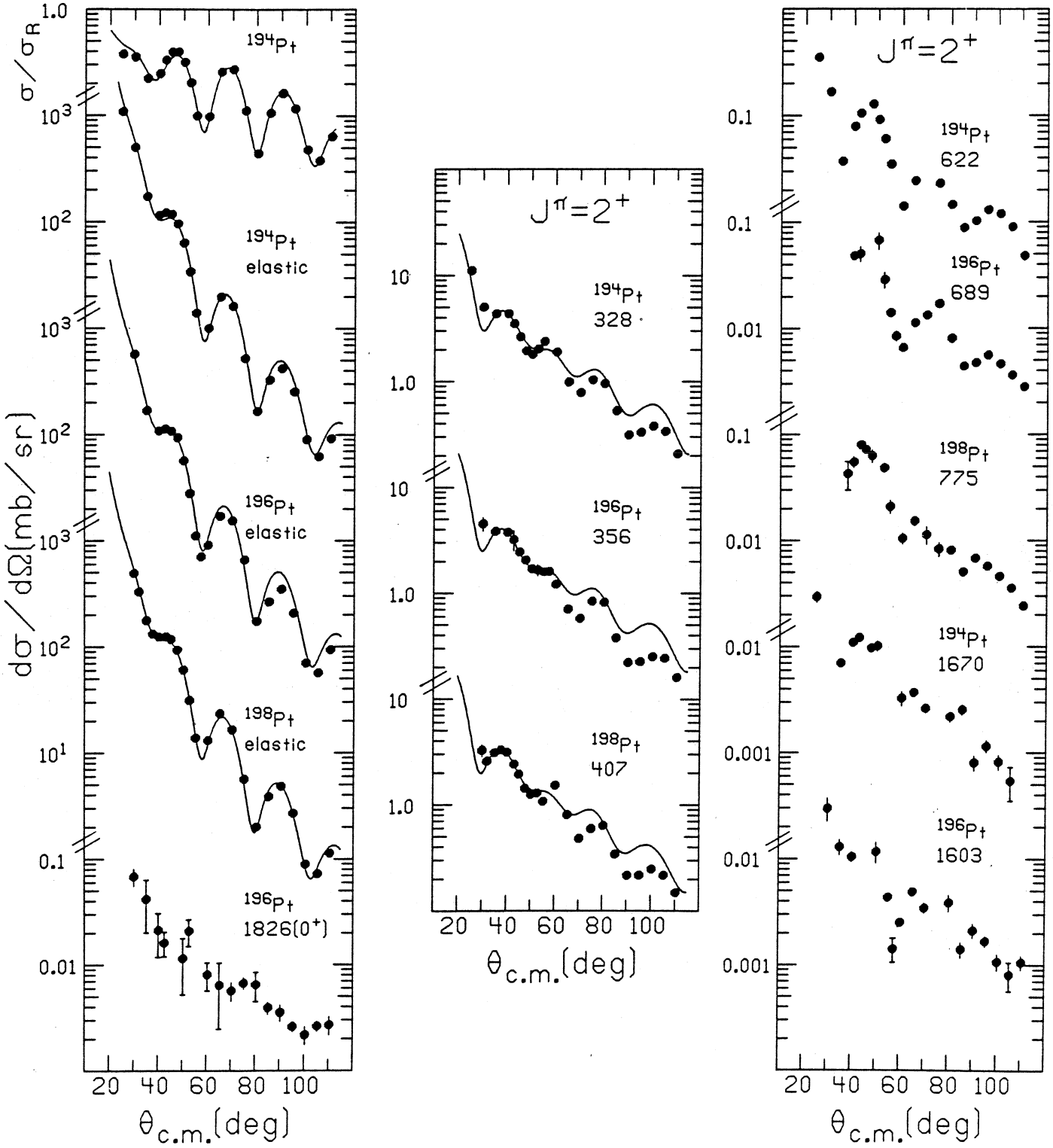

"A Study of the ^{194,196,198}Pt(p,p')...," P.T. Deason et al. Fig. 3 .

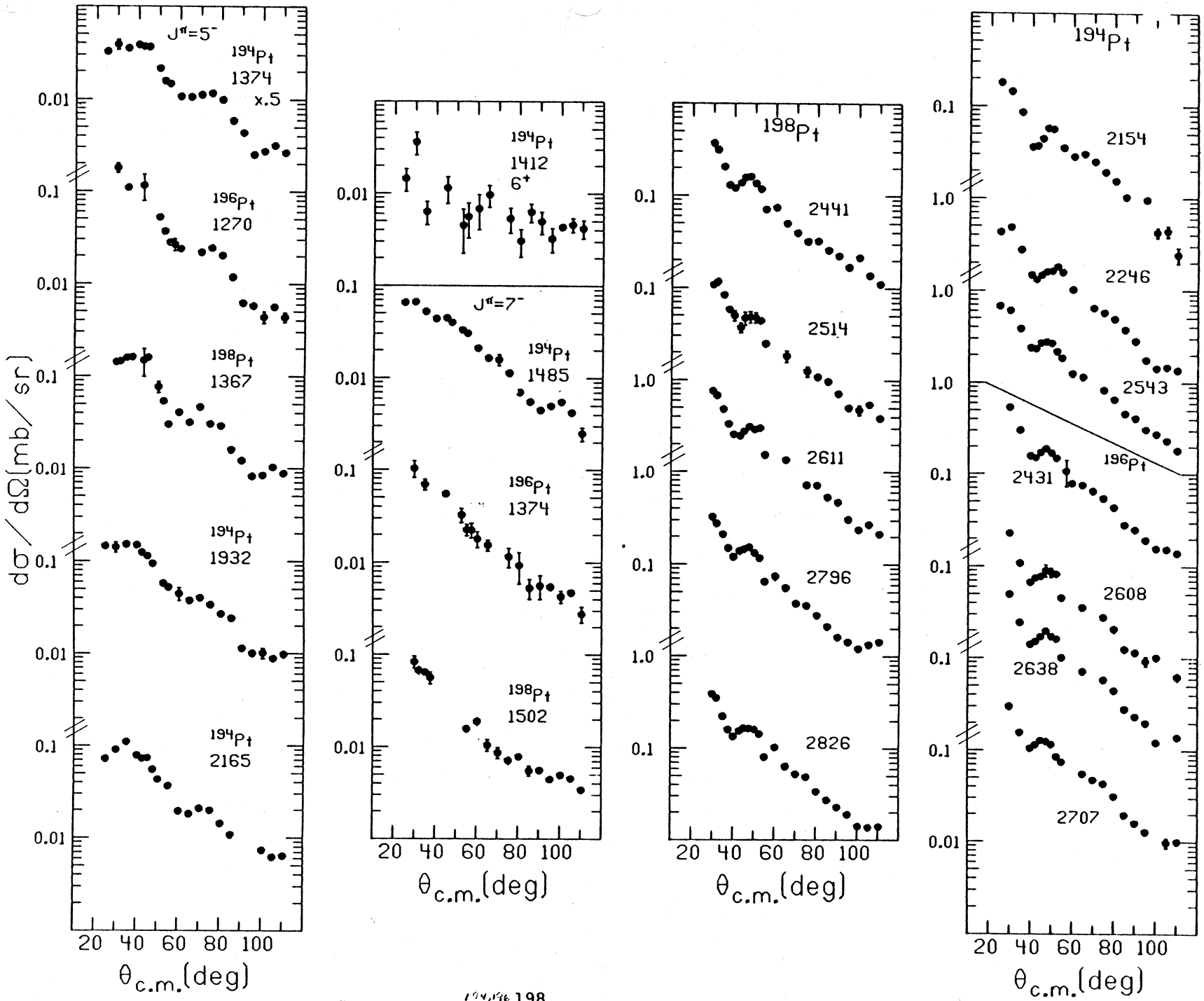

"A Study of the ^{194,196,198}Pt(p,p')...," P.T. Deason et al. Fig. 5.

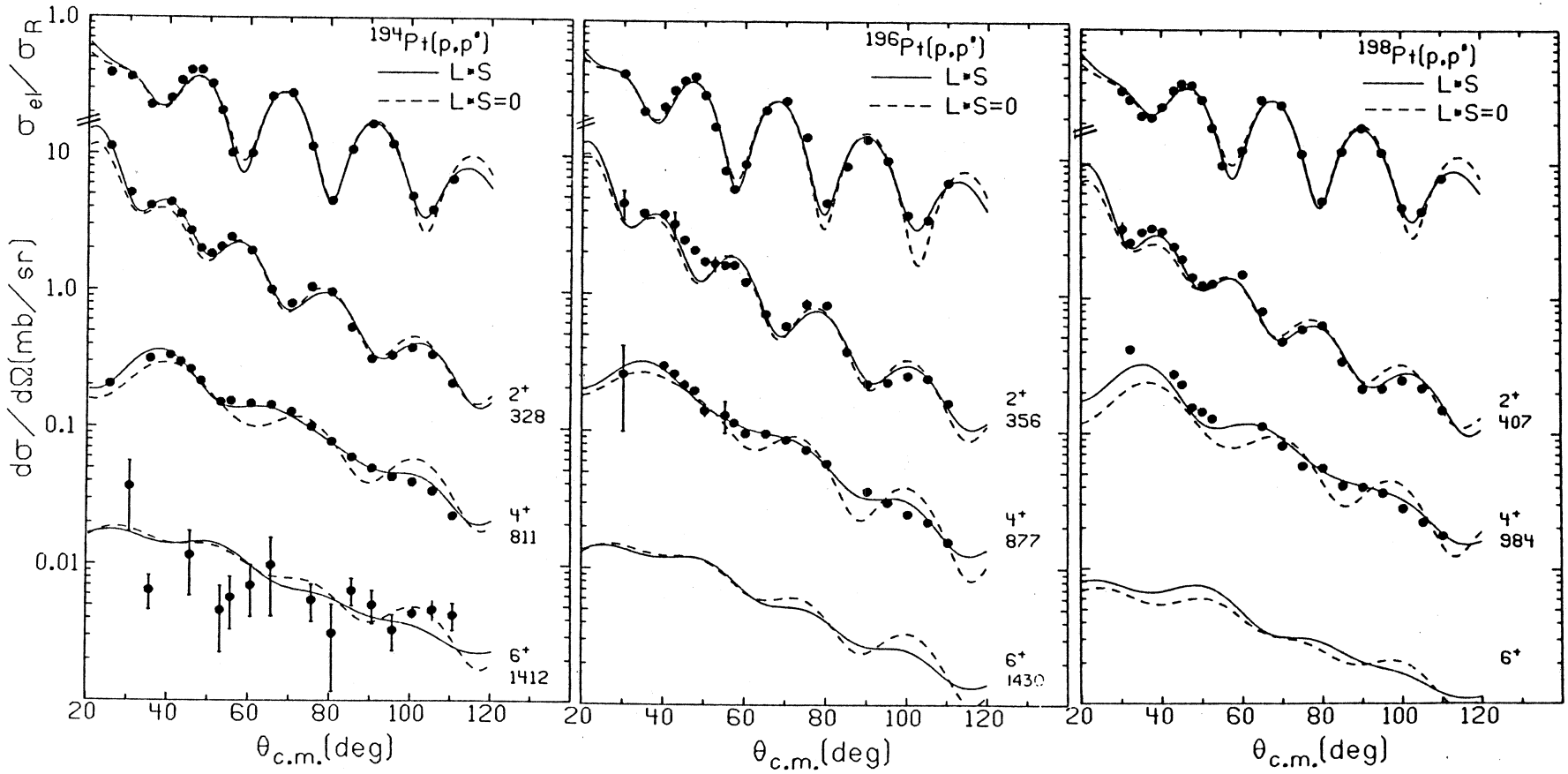

"A Study of the ^{194,196,198}Pt(p,p')...," P.T. Deason et al. Fig. 7.

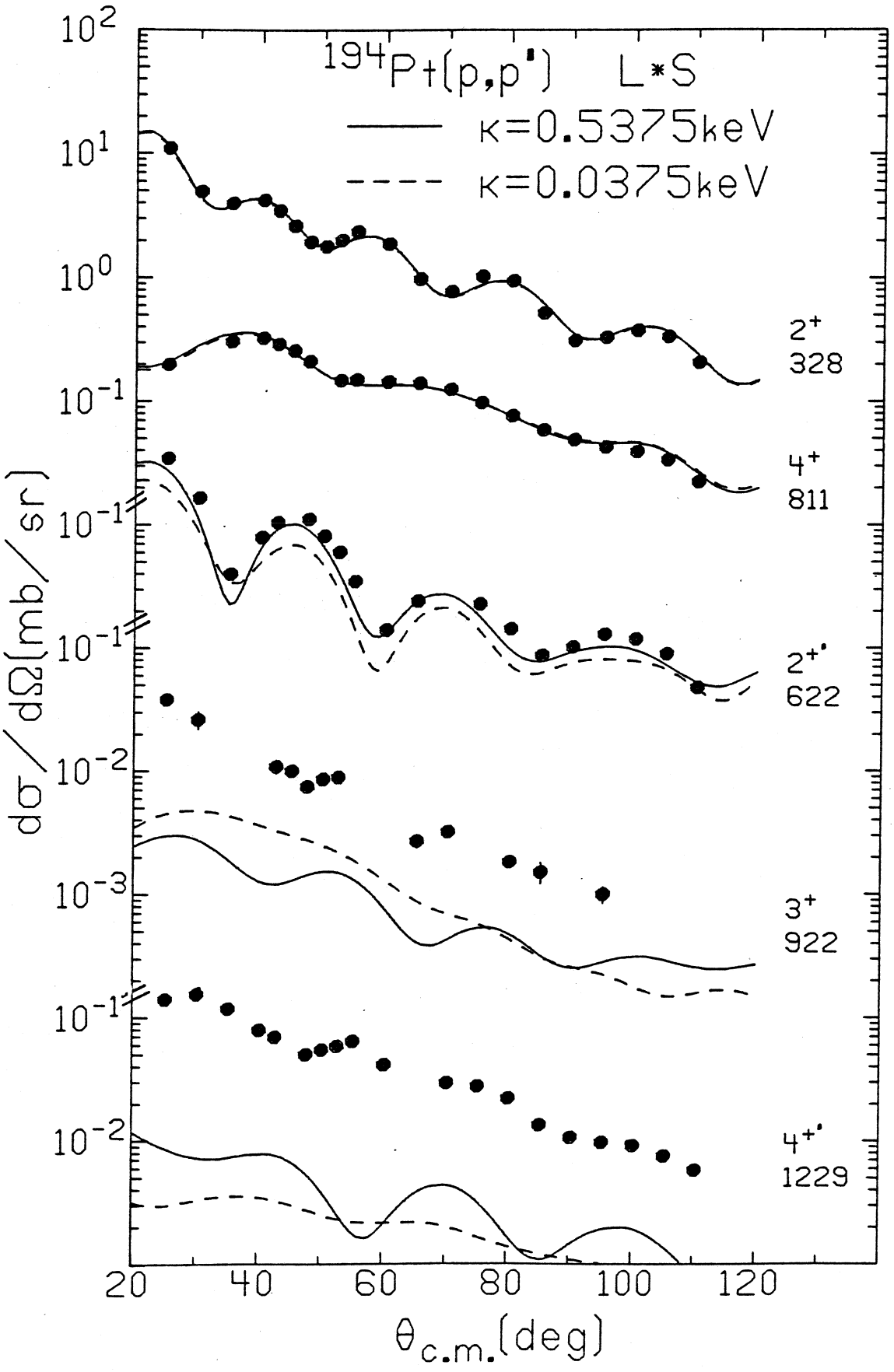

[illegible] Beeson et al. Fig. 9.

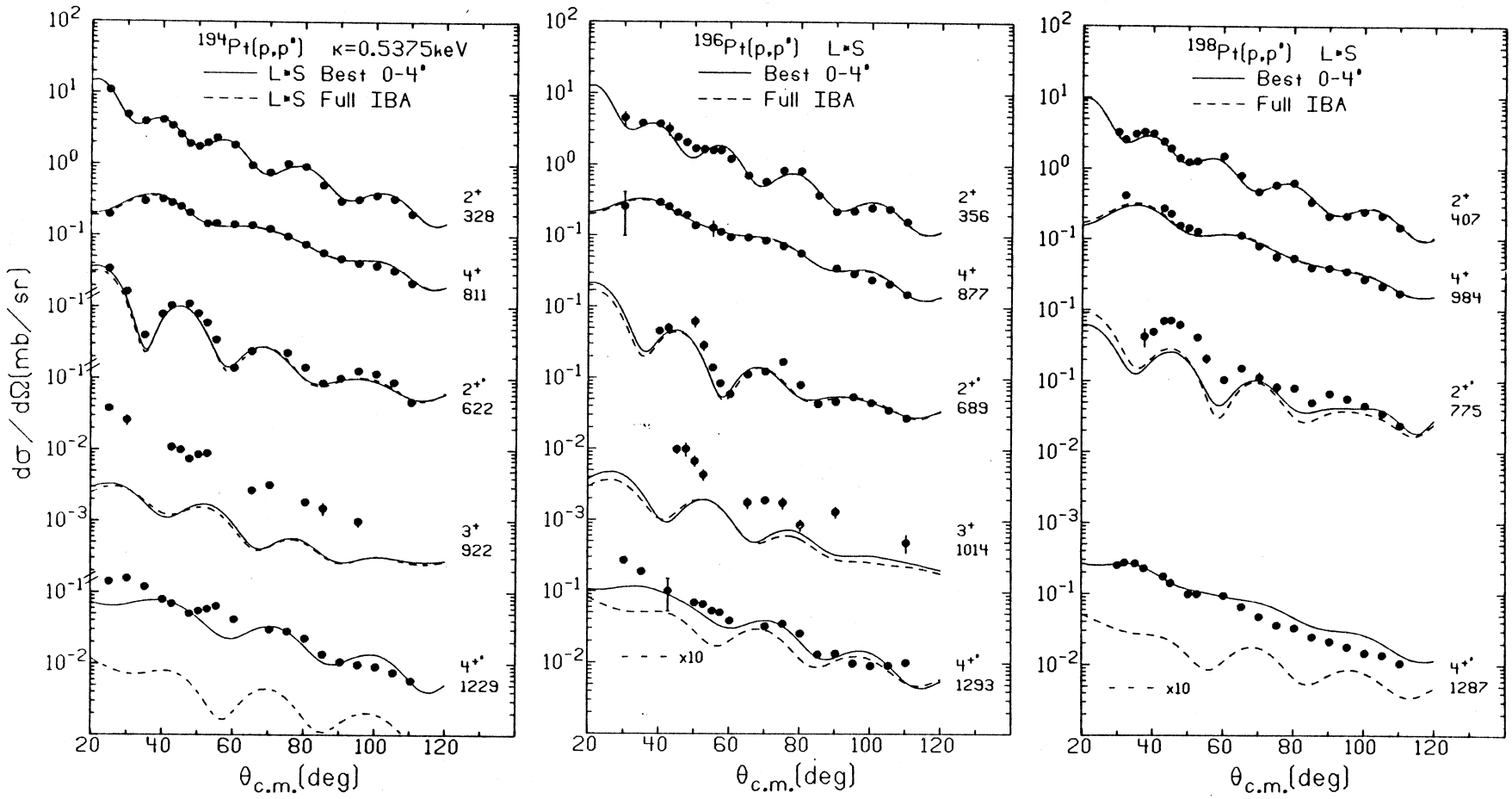

"A Study of the ^{194,196,198}Pt(p,p')...," P.T. Deason et al. Fig. 11.